Astron. Astrophys. 266, 283–290 (1992)

ASTRONOMY
AND
ASTROPHYSICS

The spectral variability in 2–28 keV of GS2023+338 during its 1989 outburst

J.J.M. in 't Zand[1], H.C. Pan[2], J.A.M. Bleeker[1], G.K. Skinner[2], M.R. Gilfanov[3], and R.A. Sunyaev[3]

[1] SRON - Laboratory for Space Research, Sorbonnelaan 2, NL-3584 CA Utrecht, The Netherlands
[2] School of Physics and Space Research, University of Birmingham, Edgbaston, Birmingham B15 2TT, U.K.
[3] Space Research Institute, Profsoyuznaya 88/32, Moscow 117296, Russia

Received May 13, accepted August 13, 1992

Abstract. The X-ray transient GS2023+338 (=V404 Cyg in the optical band), a close binary containing a black hole candidate, was observed with the coded mask X-ray camera *TTM* of the *Röntgen* observatory on the *Kvant* module of *Mir* during June–August 1989, when it was in outburst. We report here the results of an analysis of these observations, which mainly addresses the SPECTRAL variability of the transient on time scales between minutes and months.

The spectral signatures of this variability were found to consist of a fluctuating low-energy absorption with a time scale of $\sim 1\frac{1}{2}$ h, whose amplitude decreased on a time scale of ~ 1 month, and a slowly decreasing Compton-reflected component, on top of a power-law spectrum with essentially a constant photon index of 1.6–1.7. The fluctuating low-energy absorption could be satisfactory modeled by a varying column density of cold matter, with a dynamical range of at least a factor of ~ 40 and ranging up to $N_H \approx 4.5 \times 10^{23}$ H cm^{-2}. This variability most probably originated in dynamical processes. Apart from spectral variability, a wavelength-independent variability is apparent, which had time scales down to at least minutes, on top of a general decay with an e-folding decay time of 32 days. The long-term trends suggest that the environment of the compact object became progressively more transparent by accretion of the circumstellar matter onto the compact object. The total mass transferred to the compact object during the complete outburst was, through equivalence with the radiated energy during the total outburst, found to be $\sim 2 \times 10^{-9}$ $(D/1 \text{ kpc})^2$ $M_\odot$. This is equivalent to an average mass transfer rate from the companion during the quiescent stage since the last outburst of the optical counterpart of $(4\text{–}12) \times 10^{15}$ $(D/1 \text{ kpc})^2$ g s^{-1}, which is similar to that observed in other transient low-mass X-ray binaries, as long as $D < 3$ kpc.

In many of its spectral aspects, GS2023+338 resembles the galactic black hole candidate Cyg X-1 in its 'hard' state.

Key words: accretion, accretion disks – black holes – novae and cataclysmic variables – V404 Cyg – X-rays: stars

Send offprint requests to: J.J.M. in 't Zand

1. Introduction

On May 21st, 1989 the X-ray transient GS2023+338 was discovered with the All-Sky Monitor (ASM) onboard the *Ginga* satellite (Makino 1989). A few days later, this transient was identified with V404 Cyg (Wagner et al. 1989a), an optical nova known to have erupted in 1938 (Wachman 1948), 1956 and possibly 1979 (Richter 1989), indicating a recurrence time of less than about 20 years. Given a distance of >1.5 kpc (Charles et al. 1989) and the large X-ray brightness (up to 21 Crab units in the band 1–37 keV, Tanaka 1989) it became clear that GS2023+338 must involve a low-mass X-ray binary (LMXB), containing a compact object which is either a neutron star or a black hole, and a low-mass, possibly evolved, primary.

The X-ray behavior during the 1989 outburst, as observed with instruments on the *Ginga* satellite (Kitamoto et al. 1989; Tanaka 1989) and the *Röntgen* observatory onboard the manned space station *Mir* (Sunyaev et al. 1991), was unique for a transient source in two respects. Firstly, the intensity of the X-ray source exhibited strong variability on all measured time scales (down to 2 ms), with extreme jumps of up to a factor of 500 within one minute. Secondly, the X-ray spectrum showed large variations in shape, particularly during the first 10 days. Modelling the spectrum with a power-law, Kitamoto et al. (1989) found the photon-index to change from 0.00 on May 21st, via –2.5 on May 23rd to -1.4 after June 1st. Furthermore, largely variable and complex absorption was seen. The trends as seen in the X-ray lightcurve (Kitamoto et al. 1989; Kitamoto 1990) are fairly well reproduced in the optical lightcurve, strongly suggesting that the optical light originated from reprocessing of X-rays in matter surrounding the compact object (Wagner et al. 1991).

Because of the resemblance between the rapid variability seen in GS2023+338 and that in the black hole candidate (BHC) Cyg X-1 (in its 'hard state'), Tanaka (1989) suggested the possibility of a new BHC in GS2023+338. This suggestion was also supported by the very hard spectrum (up to 300 keV) observed (Sunyaev et al. 1991). Several attempts were made by a number of authors to find (orbital) periodicities in the lightcurve (e.g. Wagner et al. 1991; Gotthelf et al. 1991; Udalski & Kaluzny 1991; Leibowitz et al. 1991) and the radial velocity curve (e.g. Haswell & Shafter 1990; Casares et al. 1991; Wagner et al. 1989b) to infer orbital parameters of the system, and hence to obtain a handle on the compact object's mass. Only recently Casares et al. (1992) have succeeded in measuring beyond any doubt the radial veloc-

Table 1. Log of *TTM*-observations on the GS2023+338 field

Date (1989)	Number of observations[a]	Exposure time[b]
June 8	3	3800
June 9	4	4990
June 10	7[r]	3190
June 15	3	750[c]
July 6	4	3860
July 7	4	4470
July 8	6[r]	2120
July 9	5[r]	1860
July 10	5	6170
July 11	6	7420
August 19	6	7320
Total	53	45950

[a] One orbit defines one observation. [r] = 'rocking mode' observation, which results in about half the usual exposure time on the target.
[b] Combined exposure time for each date in seconds.
[c] Due to eclipses by the Earth, the effective exposure time on the object was limited in these observations.

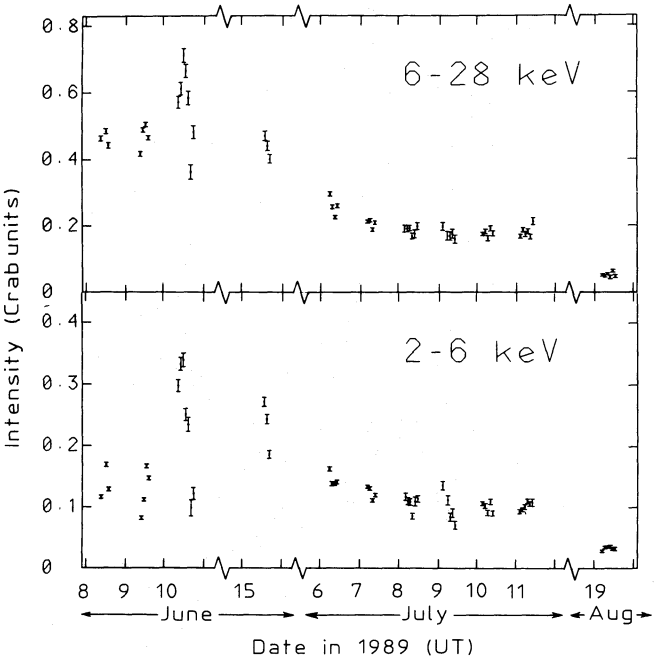

Fig. 1. *TTM*-lightcurves of GS2023+338 in two separate passbands. Intensities are expressed in Crab units (i.e. normalized on the countrate for the Crab in the same energy interval) and the time resolution is one *Mir* orbit. Times are given in UT for the center of each orbit. Note the jumps in the time axis

ity curve of the companion star with data obtained in the summer of 1991, when the optical light was not dominated anymore by reprocessed X-rays. They found an orbital period of 6.5 days and a lower limit to the compact object's mass of 6.26 $M_\odot$, making this the best BHC yet.

The X-ray instruments of the *Röntgen*-observatory on the *Kvant* module of the manned space station *Mir*, which cover a wide photon energy range of 2 till 300 keV, have made measurements of GS2023+338 during June-August 1989. These measurements have been presented already in a paper by Sunyaev et al. (1991). The work reported in the present paper involves an extension to that presented by Sunyaev et al., i.e. a more detailed assessment is made of the spectral variability of GS2023+338, employing data in the 2–28 keV band.

2. Observations

The observations discussed here were performed with *TTM*, a coded mask X-ray camera that is part of the *Röntgen* observatory onboard the *Kvant* module of the manned space station *Mir*. *TTM* was built jointly by the SRON-Laboratory for Space Research Utrecht and the University of Birmingham and is operated in collaboration with the Space Research Institute, Moscow. This camera images 8 × 8 square degrees full-width at half-maximum (FWHM) of the sky with an angular resolution of 2 arcminutes FWHM. The detector is a 95% Xenon filled position-sensitive proportional counter with a geometric open area of 540 cm^2 and sensitive between 2 and 30 keV with an energy resolution of 18% FWHM at 6 keV. For a more complete description of *TTM* we refer to In 't Zand et al. (1988). It is important to note that the sensitivity of a coded mask camera is not only determined by the detector efficiency, but also by the configuration of celestial X-ray sources in the observed part of the sky; in short, there is cross-talk between X-ray sources. Specifically for the GS2023+338 field this means that the sensitivity is somewhat suppressed by the presence of the nearby (bright) sources Cyg X-1 and Cyg X-3.

In general, the *Röntgen* observatory (Sunyaev et al. 1987) can perform observations for 10 to 30 minutes during the low environmental background period of each $1\frac{1}{2}$ hour orbit. During 11 days in 1989, between June 8th and August 19th, 53 orbits were devoted to observations of GS2023+338. In total the source was observed for about 13 hours. Table 1 presents a log of the *TTM* observations on GS2023+338.

3. The data: lightcurve and spectrum

Lightcurves, as measured by *TTM* in the 2–6 and 6–28 keV bands, are shown in Fig. 1 with a time resolution of 1 *Mir* orbit. Several interesting phenomena may be inferred from this:

1. within a time span of slightly more than two months, the average X-ray brightness between 2 and 28 keV declined with a factor of 7, corresponding to an e-folding decay time of ~35 days;
2. there is considerable variability from measurement to measurement, up to a factor of 2 in intensity;
3. the variability is much stronger in the low energy band than in the high energy band, particularly in June.

The latter aspect is very clear from Fig. 2, which shows combined spectra from 2 days of observation in June, indicating a large fluctuation in the low-energy part of the spectrum. This was already noted by Tanaka (1989) and Sunyaev et al. (1991). It is also apparent from Fig. 2 that the spectra are complex. The complexity observed in these data has already been indicated by Sunyaev et al. (1991). They found that the June spectra contain breaks in the 2–28 keV range near 4–5 keV and 9–10 keV and

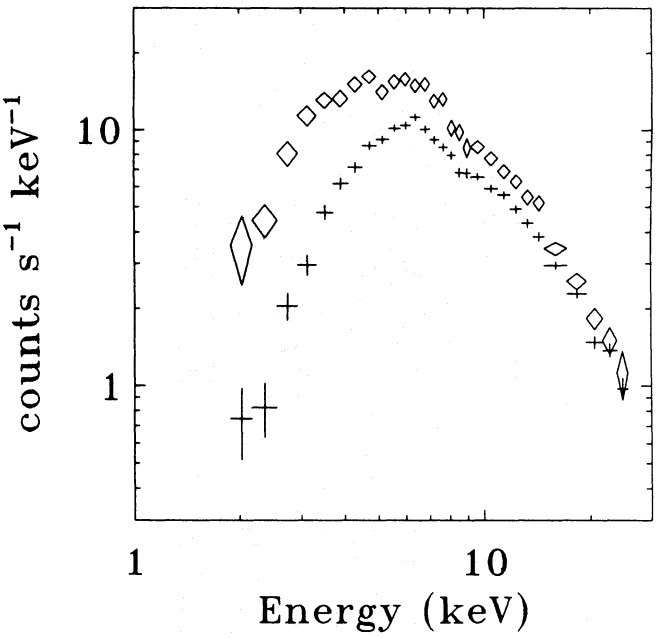

Fig. 2. Average count-spectra of GS2023+338 for two days of observation in 1989: June 8th (crosses) and 10th (diamonds)

suggest that these may be due to an integrated contribution of emission originating in different zones of an accretion disk with different temperatures. In this paper a model is proposed for this spectral structure. The prominent spectral structure, present in the June spectra, is less obvious at later dates.

4. Spectral variability

4.1. Analysis method

From the rough analysis, discussed above, it is clear that the data suggest two types of spectral variability: a fast and strongly fluctuating low-energy modulation and an apparently slower change in the remaining part of the spectrum. To model the observed spectral variability, we choose to employ an empirical approach. In this approach we first try to solely fit the modulation of the low-energy component without as yet making any model assumption on the shape of the intrinsic spectrum (we define the 'intrinsic' spectrum to be the spectrum without low-energy modulation). This method, if successful, potentially allows the study of spectral properties other than the low-energy modulation with higher statistical accuracy, through the combination of spectra that are corrected for the low-energy modulation, and may consequently be more restrictive towards a spectral model for the source.

In order to investigate the low-energy modulation independent from the intrinsic spectrum, we developed the method of differential absorption measurement. In this method, it is assumed a priori that the intrinsic spectrum remains constant over the analysis period and that the varying low-energy modulation can be solely attributed to a fluctuating low-energy absorption. The associated absorption measure is determined differentially, i.e. it is analyzed how much the spectrum is absorbed at any moment relative to when the absorption was least in the whole data set.

Hence, in this method the total spectrum incident on the detector is described by

$$F(E,t) = C(t)\, e^{-\sigma(E)N_H(t)}\, F_C(E) \quad (1)$$

with $C(t)$ a time-dependent normalization factor, $\sigma(E)$ the cross section of a cold gas of cosmic abundance per H-atom (from Morrison & McCammon 1983) and $N_H(t)$ the time-dependent term of the total absorbing hydrogen column density, excluding a constant value for the interstellar matter. $F_C(E)$ represents the intrinsic spectrum. In the differential absorption measurement, $F_C(E)$ is cancelled out through division by a 'reference spectrum', thus acquiring ratio spectra. The choice of the reference spectrum is straightforward: the weighted average of those spectra that show the least low-energy absorption. Values for $N_H(t)$ and $C(t)$ derive from fits to the modulation $C(t)\ e^{-\sigma(E)N_{H(t)}}$, convolved with the response of the detector[1]. Results for Pearson's χ^2-test indicate whether the used model is correct, i.e. whether the chosen reference spectrum is indeed representative of the intrinsic spectrum, and provide a verification of the a priori assumption on the constancy of the shape of the intrinsic spectrum.

Since the intrinsic spectrum is slowly variable, it must be anticipated that different reference spectra need to be defined for several periods. The number of necessary different reference spectra follows from the χ^2-tests. It is noted that N_H and C values found for sets of ratio spectra with different reference spectra are in principle not directly comparable.

4.2. Results on GS2023+338

We applied the method of differential absorption measurement to the *TTM* data of GS2023+338, resolving the data in the highest possible time resolution permitted by the statistical quality of the data for this kind of analysis, i.e. 250 s. Only the data taken during June 8-10 were thus resolved, because only in that period heavy low-energy absorption was observed (cf. Figs. 1 and 2). Furthermore, all data were processed with a 1 *Mir*-orbit time resolution (=1½ h). Experimenting with the method of differential absorption measurement on the data of GS2023+338 resulted in the necessity to define two different reference spectra, for the June and July-August periods separately. This indicates a typical time scale of one month in the intrinsic spectral variability.

Apart from N_H and C, we also present the results with the parameter C_E, which is defined as the factor $e^{-\sigma(E)N_H(t)}$ convolved with the instrument response and integrated over the full passband; C_E indicates the relative effect of the low-energy absorption on the total 2-28 keV intensity. The results for all three parameters, as well as for the reduced value of χ^2 for the best-fit model, are presented in Fig. 3 for the one-orbit ('low') time resolution and in Fig. 4 for the 250 s ('high') time resolution. From the reduced values of χ^2 it is clear that the model generally describes the *TTM* data well. We note that the use of two different reference spectra has practically no influence on the comparability of N_H and only slightly on that of C: C=1 is equivalent to a 2-28 keV luminosity of $1.8 \times 10^{36}(D/1\ \text{kpc})^2$ erg/s in June and $1.7 \times 10^{36}(D/1\ \text{kpc})^2$ erg/s in July-August.

[1] In fact, a rough model must be used for the intrinsic spectrum in the models for the modulation by the low-energy absorption, particularly because of escape effects in the detector (see e.g. Bertin 1975, chapter 6). A power-law spectrum, roughly describing the observed spectrum, is sufficient for this.

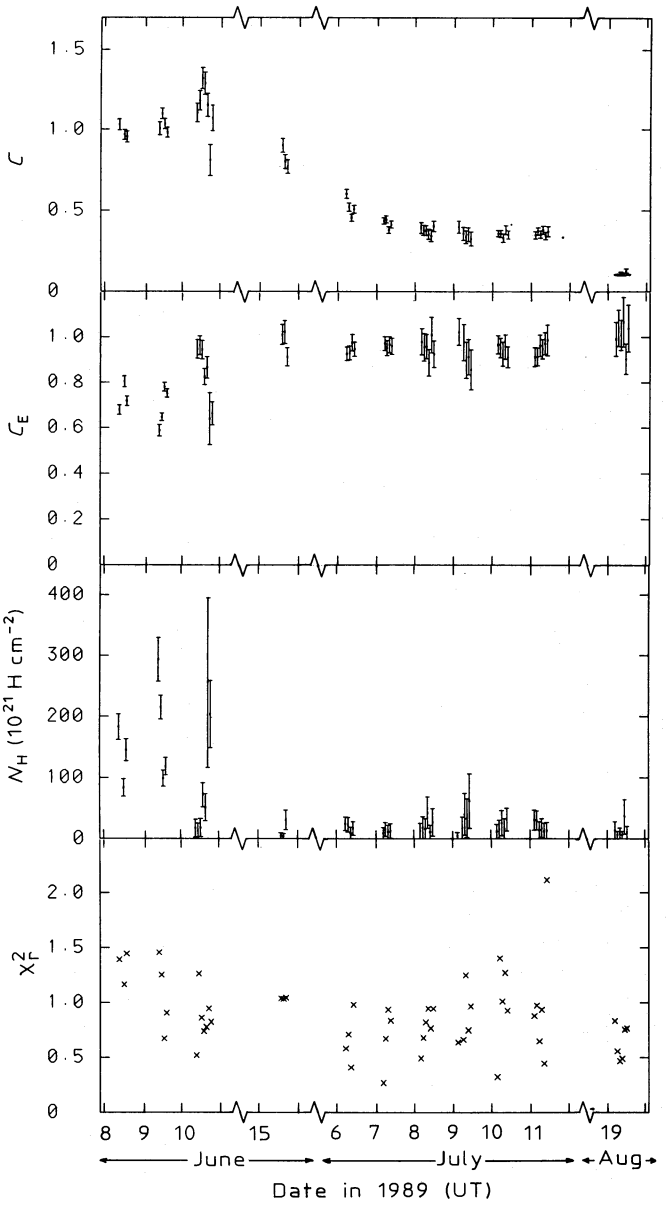

Fig. 3. Results of modelling the spectral variability of GS2023+338 with a time resolution of one *Mir* orbit (cf. Fig. 1), from top to bottom: normalized energy-independent brightness (C), fractional intensity in total passband due to absorption (C_E), the variable component of the column density (N_H in H-atoms per cm^2) and χ^2_r, the result for the statistical test of the applied model

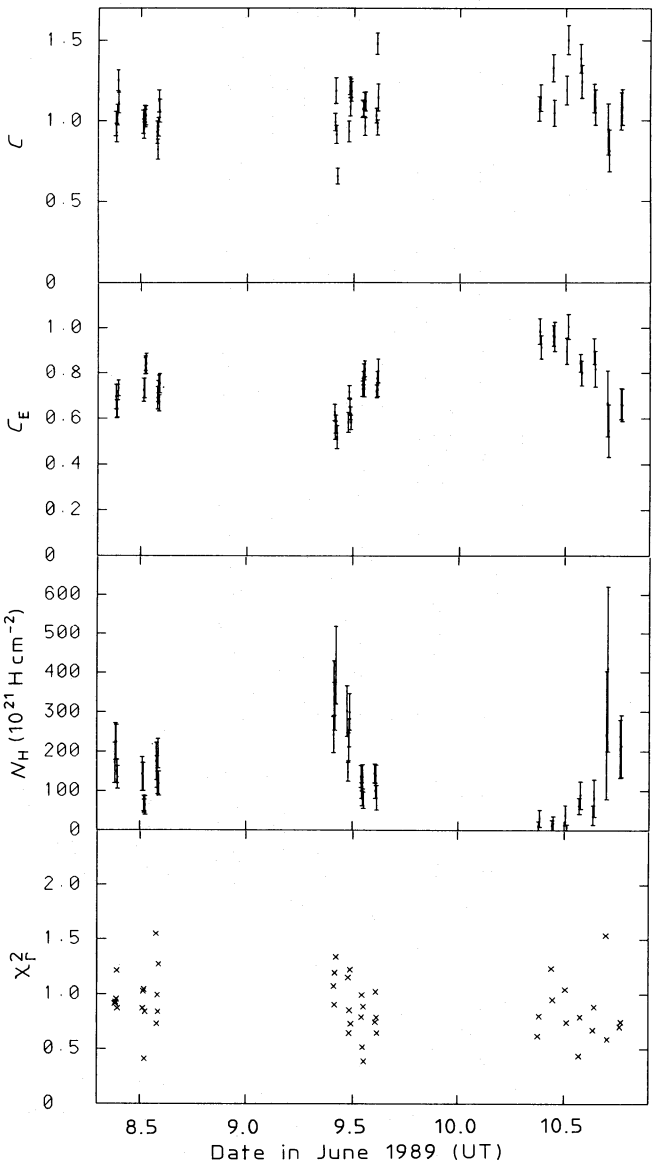

Fig. 4. Same as Fig. 3, but now with a time resolution of 250 s and only for the data obtained on June 8–10

It is evident from Figs. 3 and 4 that a strong fluctuation of N_H is present during the June observations. The N_H-values are well above the detection threshold of $\sim 10^{22}$ H-atoms per cm^2. The dynamic range in N_H was found to be at least a factor of ~40, with a maximum N_H found in the high time resolution of $(4.5 \pm 1.0) \times 10^{23}$ H-atoms per cm^2 on June 9.42394 (UT), corresponding to a maximum absorption of ~40% in the full energy band.

Evaluating the high time resolution (Fig. 4), it appears that the N_H-fluctuations do not persist towards shorter time scales: within one *Mir* orbit there is no significant fluctuation from measurement to measurement. In order to check this quantitatively, we calculated the extra spread that is present in the data on top of the statistical spread (the spread is defined here as the root mean square of the sum of the quadratic residues with respect to the weighted mean). The resulting rms values, expressed in percentages of the weighted mean, are given in Table 2. The rms value for C_E does indeed show no evidence of being larger in the high than in the low time resolution. Furthermore, this value is significant only for the June data. The fluctuations in N_H degraded in July and August with at least a factor of 10, as compared to the June period.

Regarding C, this intensity shows significant variability within the June and July data, although this variability is of a more monotonous nature in July than it is in June. Contrary to the time scale of the variability in C_E, the variability in C does show evidence for extending down to 250 s during June. Applying Pearson's χ^2 test, a <3% probability was found for the rms value to be the same in both time resolutions.

Table 2. Fractional rms values for intensities C and C_E, for all data. Upper limits are 3σ-values.

Period (1989)	Time-resolution	rms (%) in C	*rms* (%) in C_E
June 8–10	250 s	13.1 ± 1.4	13.1 ± 1.4
June 8–10	1 orbit	8.3 ± 1.7	12.1 ± 2.4
July 6–11	1 orbit	15.5 ± 2.1	<1.1
August 19	1 orbit	<3.5	<4.7

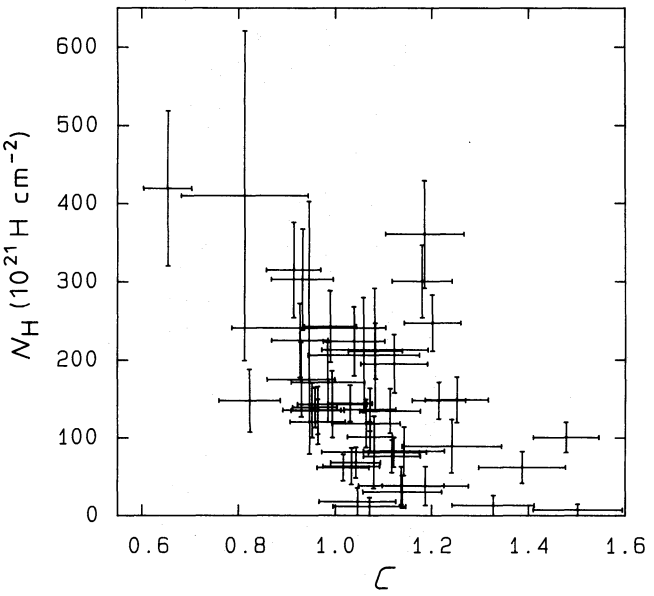

Fig. 5. The relationship between N_H and C for June 8–10 in high time resolution

Figure 5 shows the correlation between C and N_H in the June 8–10 data. The linear correlation coefficient between these two parameters in June 8-10 is -0.32, with a probability of <2% that the observed correlation occurred by chance. However, leaving out two points with extreme C values enhances the probability to < 15%, so that we conclude that the proof of correlation is only marginal.

In conclusion, the intensity variability on time scales smaller than $\sim 1\frac{1}{2}$ h can, given the quality of the data, be attributed entirely to an energy-independent variability, while on longer time scales the variability due to fluctuations in the thickness of the absorbing matter in the line of sight becomes important. Given the sampling of the data, the shape of the intrinsic spectrum does not show significant variability on time scales less than about a week.

Since we could decouple the intrinsic intensity fluctuations C from the fluctuation due to the varying low-energy absorption (which was particularly strong in June), we could determine the e-folding decay time independent from the fluctuation in the low-energy absorption. We found it to be 31.6±0.7 days, which is slightly less than the value determined from the total brightness decay.

The long-term variability of the intrinsic spectrum is illustrated in Fig. 6 where we present the estimated incident photon spectra per month of observation. These spectra are normalized

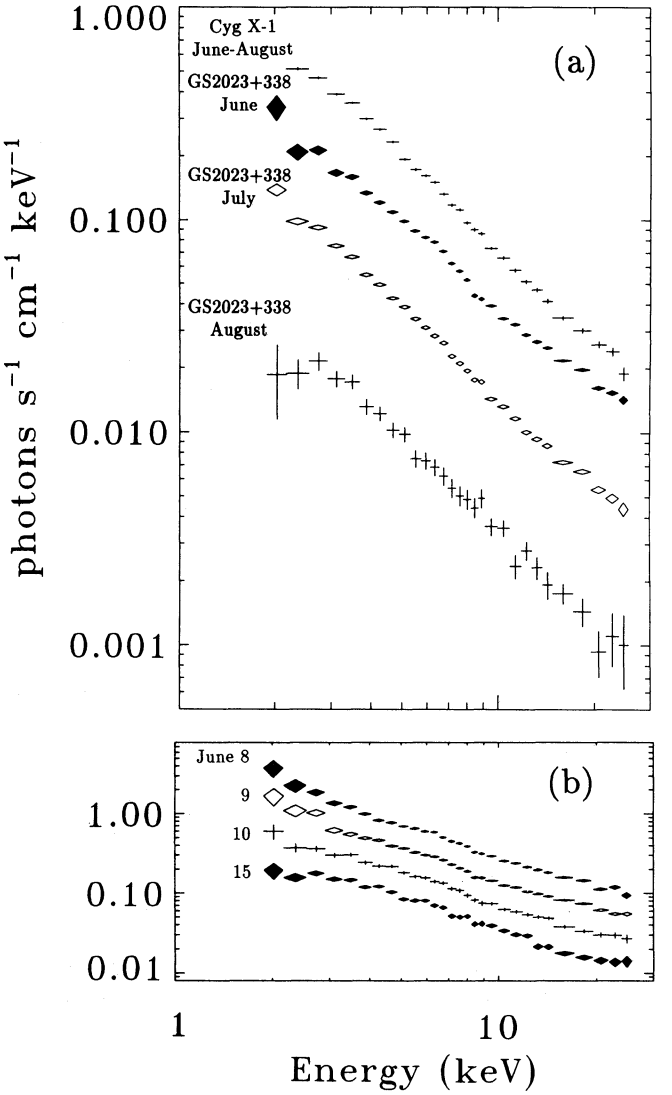

Fig. 6. a Photon spectrum of GS2023+338, corrected for absorption, separately for all observations obtained in June, July and August. For comparison we have included the spectrum of Cyg X-1, combined from 43 observations listed in Table I and offset by a factor of 2. Cyg X-1 did not show strong spectral variability during this period. **b** The intrinsic spectrum of GS2023+338 in arbitrary flux units on a daily basis during June

to the average C per period. A separate panel in Fig. 6 shows the intrinsic spectrum on a daily basis, to indicate the slow evolution of the intrinsic spectrum. Furthermore, the spectrum of Cyg X-1, as measured simultaneously with *TTM*, is shown for comparison. Figure 6 clearly demonstrates evolution in the form of the intrinsic spectrum. Characteristic in the June spectrum is a sag beyond 6–7 keV in an otherwise power-law like spectrum. The sag is also present in the July spectrum, but to a lesser degree. Such a sag was also noticed in *Ginga* data of GS2023+338 by Inoue (1989), who found this to be quite reminiscent of spectra of active galactic nuclei (AGN). AGN spectra can often be explained with a three-component model: a power-law spectrum, a component originating in Compton-reflection of the power-law spectrum against cold or slightly ionized matter and an Fe-K

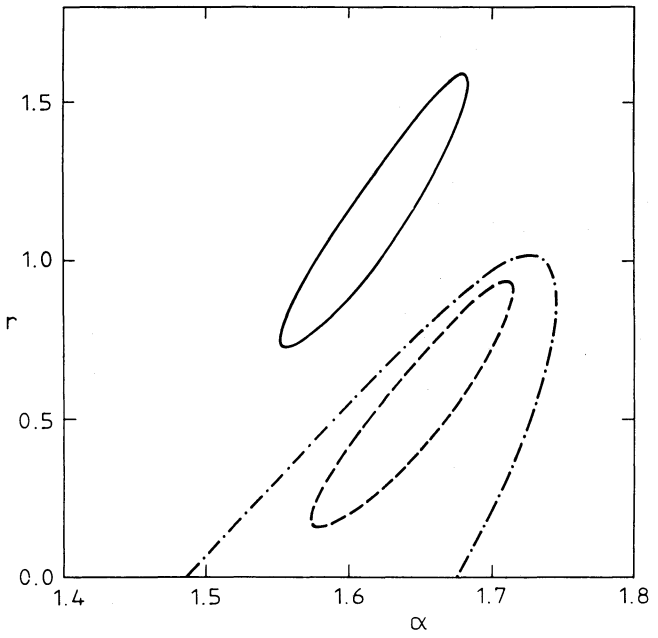

Fig. 7. 90% confidence regions for the solution of α and r, for June (solid curve), July (dashed curve) and August (dashed-dotted curve). The accompanying minimum χ^2/ν values are: 36.9/26 (June), 25.8/21 (July), 17.42/26 (August)

fluorescence line at 6.4 keV. This model may be described by:

$$F = \left(K\, E^{-\alpha}\, [1 + r\, R(E,\alpha)] + I_{\rm Fe}\right)\, e^{-\sigma(E) N_{\rm H}}$$
$$\text{photons s}^{-1}\text{cm}^{-2}\text{keV}^{-1} \qquad (2)$$

with α the photon index of the power law, $R(E,\alpha)$ the magnitude of the Compton-reflected component expressed in that of cold matter with a covering factor $\Omega/4\pi = \frac{1}{2}$, r a scaling factor, and $I_{\rm Fe}$ the flux of the iron line. The function $R(E,\alpha)$ has been specified by Lightman & White (1988) and White et al. (1988); it takes into account elastic scattering up to $\sim$ 15 keV and Compton down-scattering of hard X-rays beyond this energy.

We were able to explain the *TTM* intrinsic spectra satisfactorily with this model, as did Tanaka (1990) for *Ginga*-spectra taken earlier on in the outburst (in late May 1989). In order to do so, we kept the column density of the interstellar matter at a value of 6×10^{21} H-atoms cm^{-2}, consistent with the amount of reddening observed in the optical spectrum (Charles et al. 1989). Furthermore, we used the function $R(E,\alpha)$ applicable to slightly ionized material (i.e. $\xi_0 = 0.02$, with ξ_0 the ionization parameter as defined by Lightman & White 1988). Fits with the model to the intrinsic spectrum per month of observation revealed that the spectrum evolves to a smaller reflection component, while the power-law index remains essentially constant at a value of $\alpha = 1.6 - 1.7$ (see Fig. 7 for confidence regions in α/r parameter space, and Fig. 8 for the best fit to the intrinsic June spectrum). The fraction of the total 2-28 keV luminosity produced by the reflected component decreased from 0.19 ± 0.02 in June, via 0.11 ± 0.02 in July to an upper limit of 0.08 in August (errors are 1σ).

We also applied the above-mentioned spectral model to the Cyg X-1 spectrum shown in Fig. 6. The Cyg X-1 spectrum also shows a significant amount of Compton-reflection and a power-law index similar to that of GS2023+338. The best fit parameters for this spectrum are: $r = 0.4 \pm 0.1$ and $\alpha = 1.70 \pm 0.04$ (χ^2/ν=57.2/26).

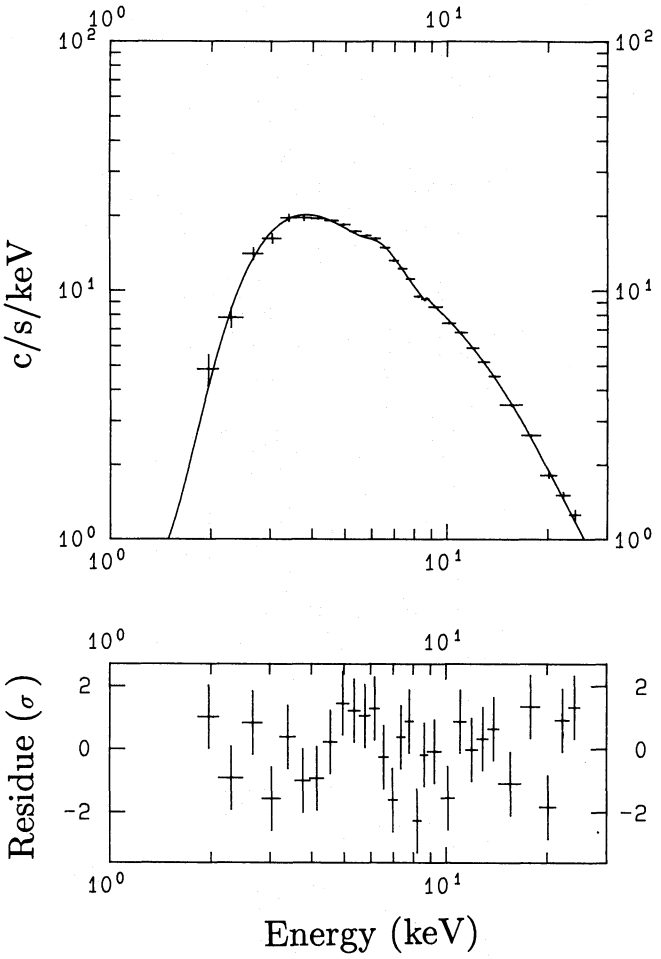

Fig. 8. Best-fit model spectrum (according to Eq.2) to the intrinsic count-spectrum of June ($\alpha = 1.60$, $r = 1.0$)

5. Discussion

With a time resolution of 250 s, the maximum luminosity within the *TTM* passband was found on June 10.51113 (center of time bin in UT) at a level of 2.8×10^{36} $(D/1\ \text{kpc})^2$ erg/s (corrected for circumstellar absorption). One may extend this result to 300 keV, by using the results found with other instrument aboard *Röntgen* (Sunyaev et al. 1991), to $\sim 11 \times 10^{36}$ $(D/1\ \text{kpc})^2$ erg/s. This is less than the Eddington limit for a compact object mass larger than 6.26 $M_\odot$ (8×10^{38} erg/s), as long as $D \lesssim 9$ kpc. Given the distance estimate of Charles et al. (1989) of 1.5–3 kpc, a near-Eddington luminosity can be ruled out for this period. However, during the *Ginga* observations of late May the source was observed to be about 50 times as bright and a near-Eddington luminosity could very well have occurred (Tanaka 1989). The assumption of a near-Eddington luminosity for GS2023+338 is supported by evidence for a 1–37 keV flux saturation on May 30th at a level of 1.5×10^{38} $(D/1\ \text{kpc})^2$ erg/s (Tanaka 1989).

GS2023+338 is different from other X-ray transient BHCs in the sense that its spectrum never showed evidence for a blackbody (BB) component, commonly seen in 2–30 keV spectra of

LMXBs and ascribed to thermal emission from an accretion disk. We found an upper limit to the bolometric flux of a BB component with $kT = 1$ keV of $< 1.4 \times 10^{-11}$ erg s^{-1} cm^{-2} (within the *TTM* passband this amounts to $< 6 \times 10^{-4}$ times the total measured flux). The lack of a BB component is also observed in two BHCs whose X-ray emissions are persistent: Cyg X-1 and GX339-4 during their 'hard' spectral state (these sources switch from time to time to an 'ultra-soft' spectral state, during which they do show a BB component). As Tanaka (1990) noted, the presence of a BB component is not uniquely given by the mass accretion rate. Whether other parameters are important is not clear; certainly the inclination angle is not, because of the bimodal behavior of Cyg X-1 and GX339-4. For some reason the accretion disk seems to extend less far down to the compact object during the hard state than during the ultra-soft state.

GS2023+338 is exceptional among transient BHCs for yet another reason: its strong N_H fluctuation in the first month of the outburst. Such a feature is, among LMXBs, only observed in dipping sources with comparable N_H values (see Parmar & White 1988 for a review). Dips in the X-ray flux are presumably caused by irregularities in an accretion disk that occasionally obstruct the line of sight during their orbital motion. Dips have also been seen in Cyg X-1 (see e.g. Bałucińska & Hasinger 1991). A dip-like origin for the low-energy absorption in GS2023+338 does not seem probable, because the duration of the absorption relative to the orbital period far exceeds the usual value for dips. A dynamical origin, however, seems likely, given the near-Eddington luminosity in the early stages of the outburst. Such a luminosity may well have provided a rather inhomogeneous environment to the compact object, with a range of different densities. If we interpret the $1\frac{1}{2}$ h time scale as due to Keplerian motion, the dynamical parameters given by Casares et al. (1992) yield a lower limit for the distance between the absorbing material and the compact object of $\gtrsim 8 \times 10^{10}$ cm. For comparison, the distance between both binary components is $(1.9-2.8) \times 10^{12}$ cm. This result is consistent with the absence of a BB component: the lower limit is far greater than the innermost radius of a stable accretion disk, i.e. 3 Schwarzschild radii (equivalent to 10^7 cm for a 10 $M_\odot$ black hole), where most of the accretion-disk BB radiation within the *TTM* passband would potentially originate.

The slight correlation between N_H and C (cf. Fig. 5) suggests that, apart from a dynamical origin, the fluctuation in low-energy absorption on June 8–10 might also be explained in terms of photo ionization (rather than N_H, the cross section $\sigma(E)$ fluctuates). We will consider this possibility briefly. Full ionization of all relevant elements up to iron requires the ionization parameter $\xi = L_x/nd^2$ to be at least 10^4 (e.g. Kallman & McCray 1982), where n is the particle density and d the distance to the source. If we assume $n = 1.4N_H/d$ (for cosmic abundances) with $N_H = 4.5 \times 10^{23}$ cm^{-2} and take for L_x the maximum possible value (2×10^{38} erg/s as dictated by the equivalence of the saturated luminosity level, found by Tanaka 1989, to the Eddington luminosity of a 20 $M_\odot$ object and the maximum luminosity found from *TTM* data), we find an upper limit for the radius within which the radiation can fully ionize the environment: $d \lesssim 4 \times 10^{10}$ cm. The longest time scale expected for bremsstrahlung cooling of such a plasma, with $T = 10^7$ K, is $\sim$ 1 minute. This is two orders of magnitude shorter than the time scales observed. In view of the fast variability of the source flux, an explanation of the observed fluctuation in low-energy absorption in terms of photo ionization therefore seems less likely.

Apart from the general decrease in low-energy absorption, the spectral variability of GS2023+338 at time scales of the order of one week to one month is further characterized by a decrease of the reflected component. The question arises whether these tendencies are linked to a single physical process. As was noted previously (e.g. by Sunyaev et al. 1991 and Inoue 1989), the X-ray characteristics of both GS2023+338 and Cyg X-1 are reminiscent of those of active galactic nuclei (AGN). In AGNs, matter is thought to comprise basically two coexisting components that are important in the formation of the X-ray spectrum (see e.g. Lightman & White 1988): cold (thermal, $kT \sim 10$ eV) and hot (non-thermal) matter. Often these two components are envisaged as an accretion disk and a surrounding corona, but theory does not require such a geometry.

The AGN picture may also apply to galactic BHCs, such as GS2023+338 and Cyg X-1 in its 'hard' state, except that the compact object's mass is a factor $\sim 10^7$ smaller, thus the dynamical time scales and the luminosity are accordingly smaller, while the cold matter may be hotter. The sag and the hard tail in the GS2023+338 spectrum is certainly indicative of reflection against cold matter, as indicated by the quality of the spectral fits. It seems conceivable that the low-energy absorbing material represents a cold matter component against which the power-law spectrum is Compton-reflected. This would conveniently explain the coupling in the data between the decrease in the magnitude of the reflected component and the decrease in the general level of low-energy absorption, both potentially arising from a decrease in the amount of cold matter. The general decrease in the observed values of N_H indicates a decrease of a factor of ~ 10 in the mass of the circumstellar matter from June to August.

Assuming that all gravitational energy released by the inflow of matter on the compact object was transformed into radiation, we find from the total amount of radiated energy during the whole outburst an equivalent mass of $\sim 2 \times 10^{-9}$ $M_\odot$ $(D/1 \text{ kpc})^2$. If this amount was transferred from the companion during the past quiescent stage of the X-ray transient (since the previous outburst of its optical counterpart 10 to 30 years ago, see introduction) and stored up until the 1989 outburst, the average mass transfer rate during quiescence would have been $(4–12) \times 10^{15}$ $(D/1 \text{ kpc})^2$ g s^{-1}. This value is comparable with that observed in other LMXB transient sources (e.g. White et al. 1984), as long as $D < 3$ kpc.

We also observed Compton-reflection in the spectrum of Cyg X-1, which was simultaneously measured with GS2023+338. This confirms results obtained with *Ginga* (Tanaka 1990) and represents yet another aspect of the similarity between both sources. The difference between Cyg X-1 and GS2023+338 could be that in Cyg X-1 the Compton-reflection takes place against a stable accretion disk, while in GS2023+338 it predominantly takes place against cold clumpy material, expelled earlier during a near-Eddington luminosity phase.

Finally, we note that the variability in the Compton-reflected component causes apparent changes in the power-law index if Compton-reflection is not taken into account during the spectral modelling of the data. This is clear from Fig. 6: the power-law spectrum of June appears to be harder than that of the other two months. However, the full spectral modelling is consistent with a constant power-law index. We suggest that this effect may partly be responsible for the strong index changes seen in early *Ginga*-ASM data (Kitamoto et al. 1989).

6. Conclusion

In this study we have investigated the spectral variability of the X-ray transient and BHC GS2023+338 on time scales > 250 s during June-August 1989. The spectral signatures of this variability include a fluctuating low-energy absorption with a time scale of $\sim 1\frac{1}{2}$ h and a slowly decreasing Compton-reflected component, on top of a power-law spectrum with essentially a constant index, but a variable intensity. The data can be satisfactory modeled by assuming a clumpy environment around the compact object, which gets progressively more transparent during the observations, probably by accretion of the circumstellar matter onto the compact object. The $1\frac{1}{2}$ h time scale seems to exclude photo ionization as the cause of the fluctuating low-energy absorption.

In many respects GS2023+338 resembles the BHC Cyg X-1 during its 'hard' state. Apart from the rapid intensity variability as seen with another *Röntgen* instrument (*HEXE*, Sunyaev et al. 1991), this also applies to spectral characteristics, such as power-law index, the presence of a Compton-reflected component and even, to some extent, low-energy absorption. The main difference between both BHCs, i.e. persistent versus transient behavior, may result from the different types of companion stars (an early spectral type supergiant for Cyg X-1 and a late type star for GS2023+338), because of the physical processes involved in the mass loss of these companions.

Acknowledgements. J.J.M.Z. and J.A.M.B. wish to thank F. Verbunt and J. Heise for useful discussions. Part of the research described in this paper was financially supported by the *Space Research Organization of the Netherlands* (SRON) under the auspices of the *Netherlands Organization for Scientific Research* (NWO).

References

Bałucińska, M., Hasinger, G., 1991, A&A **241**, 439
Bertin, E.P., 1975, "Principles and Practice of X-ray Spectrometric Analysis", 2nd ed., Plenum Press, New York
Casares, J., Charles, P.A., Jones, D.H.P., Rutten, R.G.M., Callanan, P.J., 1991, MNRAS **250**, 712
Casares, J., Charles, P.A., Naylor, T., 1992, Nat **355**, 614
Charles, P.A., Casares, J., Jones, D.H.P. et al., 1989, In: J. Hunt and B. Battrick (eds.) Proc. 23rd ESLAB Symp., Two Topics in X-Ray Astronomy, ESA SP-296, Noordwijk, p. 103
Gotthelf, E., Patterson, J., Stover, R.J., 1991, ApJ **374**, 340
Inoue, H., 1989, In: J. Hunt and B. Battrick (eds.) Proc. 23rd ESLAB Symp., Two Topics in X-Ray Astronomy, ESA SP-296, Noordwijk, p. 783
Haswell, C.A., Shafter, A.W., 1990, IAU Circ. 5074
In 't Zand, J.J.M., Jager, R., Heise, J. et al., 1988, In: H. Ögelman and E.P.J. van den Heuevel (eds.) Timing Neutron Stars, NATO ASI Series No. C262, Kluwer Academic Publishers, Dordrecht, p. 317
Kallman, T.R., McCray, R., 1982, ApJS **50**, 263
Kitamoto, S., Tsunemi, H., Miyamoto, S. et al., 1989, Nat **342**, 518
Kitamoto, S., 1990, In: C.W. Mauche (ed.) Proc. Workshop on Accretion-Powered Compact Binaries, Cambridge University Press, Cambridge, 21
Leibowitz, E.M., Ney, A. Drissen, L., Grandchamps, A., Moffat, A.F.J., 1991, MNRAS **250**, 385
Lightman, A.P., White, T.R., 1988, ApJ **335**, 57
Makino, F., *Ginga* team, 1989, IAU Circ. 4782
Morrison, R., McCammon, D., 1983, ApJ **270**, 119
Parmar, A.N., White, N.E., 1988, Mem. Soc. Astron. Ital. **59**, 147
Richter, G.A., 1989, IBVS, No. 3362
Sunyaev, R.A., Kaniovsky, A., Efremov, V. et al., 1987, Nat **330**, 227
Sunyaev, R.A., Kaniovsky, A., Efremov, V. et al., 1991, SvA L **17**, 123
Tanaka, Y., 1989, In: J. Hunt and B. Battrick (eds.) Proc. 23rd ESLAB Symp., Two Topics in X-Ray Astronomy, ESA SP-296, Noordwijk, p. 3
Tanaka, Y., 1990, In: A. Treves, G.C. Perola and L. Stella (eds.) Proc. Workshop on Iron Line Diagnostics in X-Ray sources, Lecture Notes in Physics 385, Springer Verlag, Berlin, p. 98
Udalski, A., Kaluzny, J., 1991, PASP **103**, 198
Wachman, A.A., 1948, Erg. Astron. Nachr. **11** (5), 42
Wagner, R.M., Starrfield, S.G., Cassatella, A., 1989a, IAU Circ. 4783
Wagner, R.M., Kreidl, T.J., Howell, S.B., Collins, G.W., Starrfield, S., 1989b, IAU Circ. 4797
Wagner, R.M., Starrfield, S.G., Howell, S.B. et al., 1991, ApJ **378**, 293
White, N.E., Kaluzienski, J.L., Swank, J.H., 1984, In: S.E. Woosley (ed.) Proc. Conf. on High Energy Transients in Astrophysics, AIP Conf. Proc. No. 115, New York, p. 31
White, T.R., Lightman, A.P., Zdziarski, A.A., 1988, ApJ **331**, 939

This article was processed by the author using Springer-Verlag LaTeX A&A style file 1990.